

# Memory effect induced macroscopic-microscopic entanglement

Qingxia Mu<sup>1,2,\*</sup>, Xinyu Zhao<sup>2,†</sup> and Ting Yu<sup>2,3‡</sup>

<sup>1</sup>*Mathematics and Physics Department, North China Electric Power University, Beijing 102206, China*

<sup>2</sup>*Center for Controlled Quantum Systems and the Department of Physics and Engineering Physics, Stevens Institute of Technology, Hoboken, New Jersey 07030, USA and*

<sup>3</sup>*Beijing Computational Science Research Center, Beijing 100094, China*

We study optomechanical entanglement between an optical cavity field and a movable mirror coupled to a non-Markovian environment. The non-Markovian quantum state diffusion (NMQSD) approach and the non-Markovian master equation are shown to be useful in investigating the entanglement generation between the cavity field and the movable mirror. The simple model presented in this paper demonstrates several interesting properties of optomechanical entanglement that are associated with environment memory effects. It is evident that the effective environment central frequency can be used to modulate the optomechanical entanglement. In addition, we show that the maximum entanglement may be achieved by properly choosing the effective detuning which is significantly dependent on the strength of the memory effect of the environment.

## I. INTRODUCTION

Macroscopic quantum coherence has a long history that may date back to the famous Schrödinger's cat paradox [1]. Although current research in quantum mechanics does not impose a strict boundary between quantum and classical realms, realising reliable microscopic-macroscopic entanglement is still a challenge due to the so-called decoherence processes which are especially severe for a macroscopic object. This explains that entanglement is most commonly observed in the microscopic world. In recent years, several attempts in establishing entanglement in the macroscopic or mesoscopic systems have been made [2–13]. In the same spirit, quantum entanglement between a microscopic object and a macroscopic object is expected to be a useful resource for the emerging quantum technology such as quantum information processing and quantum computing. In addition, a deeper understanding of the micro-macro entanglement and its decoherence process may be important for a better understanding of transition from classical to quantum realms [14, 15]. Apart from the motivation from the theoretical research activities, the latest developments in experimental entanglement generation, control and manipulation have provided a direct impetus for further explorations of this important setting based on optomechanical systems [16–21].

The radiation pressure in an optical cavity is capable of producing entanglement between the quantized cavity modes (microscopic system) and a movable mirror [22]. When the mass of the mirror is in the macroscopic scale, such an optomechanical system provides a natural testing bed for macroscopic quantum mechanical phenomena [23–29]. Theoretically, Markov Langevin equations or the corresponding master equations may be used to

deal with an optomechanical system when the environmental noises can be treated as a weak perturbation and the noisy memory effect can be ignored [30]. However, it becomes clear that, from both theoretical and experimental viewpoint, the memory effects plays a pivotal role in micro-macro entanglement dynamics in non-Markovian regimes [12, 31, 32]. Notably, a recent experimental observation [33] has explicitly shown that the heat bath coupled to the optomechanical system is in non-Markovian regimes. Moreover, the non-Markovian properties are shown to be useful in preserving optomechanical entanglement [34]. In addition, an environmental engineering technique for a non-Markovian bath demonstrated in an optical experiment [35] has suggested a promising future in manipulating non-Markovian environments to control quantum dynamics of the system of interest. Hence, it is highly desirable to develop a systematic approach to investigate the dynamics of optomechanical system in non-Markovian regime.

The purpose of this paper is to investigate the entanglement between the light field in a Fabry-Pérot cavity and one movable reflection mirror of the cavity (Fig. 1). The movable mirror is assumed to be embedded in a non-Markovian environment modeled by a bosonic bath. We shall begin our discussion with an exact quantum description of the optomechanical system consisting of cavity modes and the movable mirror. The advantage of the exact treatment is that the memory effect in this model can be treated in a systematic way without introducing any ad hoc parameters to represent the environmental noises. We shall use the non-Markovian quantum state diffusion (NMQSD) equation to solve quantum open systems coupled to a non-Markovian bosonic or fermionic environment [36–49]. Such a stochastic approach provides a very powerful tool in both analytical treatments and numerical simulations, especially in dealing with the non-Markovian perturbation and solving the corresponding master equation for the open quantum systems. With our approach, the model considered in this paper can be solved efficiently to exhibit the non-Markovian properties that affect the dynamics of optomechanical entan-

---

\* qingxiamu@ncepu.edu.cn

† xyzacademic@gmail.com

‡ Ting.Yu@stevens.edu

gement. More specifically, our results show that the environmental memory can significantly alter the speed of the optomechanical entanglement generation between the cavity field and the movable mirror. Our approach can also incorporate importantly the high frequency back reaction of the environment, which will be shown to significantly preserve the generated entanglement. Furthermore, we show that a proper choice of effective detuning is also crucial for optimizing the optomechanical entanglement.

The paper is organized as follows. In Sec. II, we present the interacting model and derive the master equation based on the NMQSD equation. Sec. III analyzes in detail the environmental memory effects on the entanglement between the mechanical mode and the intracavity mode. In particular, we show how the effective environment central frequency can be used to modulate the optomechanical entanglement. In addition, we show that the maximum entanglement may be achieved by properly choosing the effective detuning which is significantly dependent on the strength of the memory effect of the environment. Finally, we conclude the paper in Sec. IV. Some details about the equations of motions for the mean values are left to the the Appendixes.

## II. MODEL AND SOLUTION

We consider a single-sided optomechanical system, with a mechanical mode coupled to an optical mode which is driven by a coherent laser, as shown schematically in Fig. 1. The Hamiltonian of this system may be written as  $H_1 = \omega_c a_1^\dagger a_1 + \omega_m b_1^\dagger b_1 + g a_1^\dagger a_1 (b_1 + b_1^\dagger) + \Omega_d (a_1 e^{i\omega t} + a_1^\dagger e^{-i\omega t})$  [50], where  $a_1$  and  $b_1$  are annihilation operators of the cavity field and mechanical mode, with respective resonant frequencies  $\omega_c$  and  $\omega_m$ . The parameter  $g$  is the single-photon optomechanical coupling strength, and  $\Omega_d$  is the driving rate of the coherent laser with frequency  $\omega$ . We assume that the intracavity field is strong enough that the Hamiltonian can be linearized with  $a_1 \equiv a + \alpha$ ,  $b_1 \equiv b + \beta$ . Here  $a$  and  $b$  represent quantum fluctuations of optical and mechanical modes around their mean values  $\alpha$  and  $\beta$ , respectively. They are determined by  $[i(\omega - \omega_c) - ig(\beta + \beta^*) - \kappa_a]\alpha - i\Omega_d = 0$  and  $-i\omega_m\beta - ig|\alpha|^2 = 0$ , where  $\kappa_a$  is classical leakage rate of the cavity. The Hamiltonian of the system can be linearized as [20]

$$H_S = -\Delta a^\dagger a + \omega_m b^\dagger b + G(a^\dagger + a)(b^\dagger + b), \quad (1)$$

where  $G = ag$  is the effective coupling rate,  $\Delta = \omega - \omega_c + 2G^2/\omega_m$  is the optomechanical-coupling modified detuning.

We assume that the optomechanical system is coupled to a bosonic bath which can be described by a set of harmonic oscillators as

$$H_B = \sum_j \omega_j c_j^\dagger c_j, \quad (2)$$

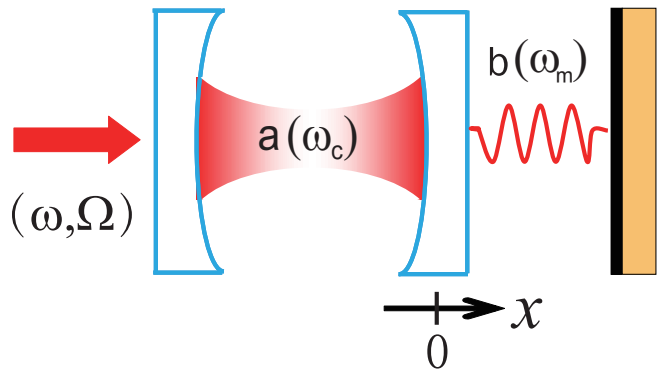


Figure 1. (color online) Schematic diagram of a typical optomechanical system, in which an optical cavity driven by a coherent laser is coupled to a mechanical mode.

where  $c_j$  and  $c_j^\dagger$  are annihilation and creation operators satisfying  $[c_j, c_{j'}^\dagger] = \delta_{j,j'}$ . The interaction between the system and the bosonic bath is given by

$$H_I = \sum_j g_j (L c_j^\dagger + L^\dagger c_j), \quad (3)$$

where  $g_j$  are the system-bath coupling strength, and  $L = b$  describing the damping of the mirror. Here, the interaction is written in a rotating wave approximation (RWA) form, a more general interaction for mirror and bath should be  $H'_I = \sum_j g_j (b + b^\dagger)(c_j^\dagger + c_j)$ . If the coupling strength is weak comparing to the system ( $g_j \ll \omega_m$ ) [51, 52], this approximation is valid. Actually the interaction  $H'_I$  can be also incorporated in the NMQSD approach. The method of solving  $H'_I$  type of interaction can be found in Ref. [40].

More general discussions on the issue may include the decoherence channels concerning the cavity leakage and the thermal damping of the mirror. For the sake of reducing technical complexity of our model, we will exclusively be focused on the vacuum environment, leaving more complete model description to the appendix A where we provide a full solution of the NMQSD equation. Our major concern in this paper is not the temperature effect on the decoherence rate, but rather on the non-Markovian properties of the environment.

Assuming that the system and the environment are initially uncorrelated, it can be proved that the state of the optomechanical system can be represented by a stochastic pure state called quantum trajectory,  $|\psi_t(z^*)\rangle$ , governed by the NMQSD equation [37, 38]

$$\partial_t |\psi_t(z^*)\rangle = \left[ -iH_S + bz_t^* - b^\dagger \int_0^t ds \alpha(t, s) \frac{\delta}{\delta z_s^*} \right] |\psi_t(z^*)\rangle, \quad (4)$$

where  $\alpha(t, s) = \sum_j |g_j|^2 e^{-i\omega_j(t-s)}$  is the environmental correlation function, and  $z_t^* = -i \sum_j g_j z_j^* e^{i\omega_j t}$  is a complex Gaussian process satisfying  $M[z_t] = M[z_t z_s] = 0$  and  $M[z_t^* z_s] = \alpha(t, s)$ . Here  $M[\cdot] \equiv \int \frac{d^2 z^2}{\pi} e^{-|z|^2} [\cdot]$  stands

for the statistical average over the noise  $z_t$ . Note that the above dynamical equation (4) contains a time-nonlocal term depending on the whole evolution history from 0 to  $t$ . For the purpose of practical applications, we can replace the functional derivative contained in Eq. (4) with a time-dependent operator  $O$  satisfying  $\frac{\delta|\psi_t(z^*)\rangle}{\delta z_s^*} = O(t, s, z^*)|\psi_t(z^*)\rangle$ . Then the NMQSD equation can be transformed to

$$\partial_t|\psi_t(z^*)\rangle = [-iH_S + bz_t^* - b^\dagger\bar{O}(t, z^*)]|\psi_t(z^*)\rangle, \quad (5)$$

where  $\bar{O}(t, z^*) \equiv \int_0^t ds \alpha(t, s)O(t, s, z^*)$  and the initial condition  $O(t, s = t, z^*) = b$  is satisfied.

It should be noted that Eq. (5) [as well as Eq. (4)] is derived directly from the microscopic Hamiltonian (1), (2), and (3) without any approximation. It is the exact dynamic equation governing the dynamics of the optomechanical system coupled to the environment, no matter the environment is in Markov or non-Markovian regime. The environmental impact on the dynamics of the optomechanical system is reflected on the terms  $bz_t^*$  and  $-b^\dagger\bar{O}(t, z^*)$  in Eq. (5). If these two terms are zero, the equation is reduced to  $\partial_t|\psi_t(z^*)\rangle = -iH_S|\psi_t(z^*)\rangle$ , which is the Schrödinger equation for the closed system. Moreover, the non-Markovian properties are reflected by the operators  $\bar{O}$  in Eq. (5). If there is no correlation between two separate time points  $t$  and  $s$ , namely  $\alpha(t, s) = \delta(t, s)$ , the operator  $\bar{O}$  is reduced to  $\bar{O} = b$ . As a result, Eq. (5) is reduced to the commonly used Markov quantum trajectory equation [53, 54]. Here, and throughout the paper, the correlation function of the environment is chosen as the Ornstein-Uhlenbeck (O-U) correlation function

$$\alpha(t, s) = \frac{\Gamma\gamma}{2} e^{-(\gamma+i\Omega)|t-s|}, \quad (6)$$

in which the parameter  $1/\gamma$  measures the memory time,  $\Gamma$  is the environmental decay rate, and  $\Omega$  is the central frequency of the environment. The O-U type correlation function corresponds to the Lorentzian spectrum density  $J(\omega) = \frac{\Gamma\gamma^2/2\pi}{(\omega-\Omega)^2+\gamma^2}$  of the environment, which has been widely used in the research on cavity optomechanics [20, 58]. A more generic correlation function or spectrum density may be needed in many other interesting situations. We would like to emphasize that our derivation is independent of a specific form of the correlation functions  $\alpha(t, s)$ , so that Eq. (5) is applicable to an arbitrary correlation function. The reason we use the O-U correlation function here is that it is convenient to observe the crossover properties of the non-Markovian and Markov transition by modulating the single parameter  $\gamma$ . If the memory time  $1/\gamma$  is very small,  $\alpha(t, s)$  is approximately reduced to  $\alpha(t, s) \approx \delta(t, s)$ , which means the environment is reduced to a Markov environment.

The key to solving the dynamic equation (5) is to find the operator  $O$ . The exact solution of  $O$  operator contains all the non-Markovian information for the environment. The exact  $O$  is also essential for the derivation of

the corresponding exact master equation. According to Refs. [37, 38],  $O$  satisfies the following equation,

$$\frac{\partial}{\partial t}O = [-iH_S + Lz_t^* - L^\dagger\bar{O}, O] - L^\dagger\frac{\delta}{\delta z_s^*}\bar{O}. \quad (7)$$

Clearly, finding the exact  $O$  operator for a particular model is not easy. Therefore, for most practical problems, of central importance of applications is the perturbation approach [39]. Notably, it is shown that the exact  $O$  operator for the model in this paper can be found,

$$O(t, s, z^*) = \sum_{j=1}^4 f_j(t, s)O_j + i \int_0^t ds' f_5(t, s, s')z_s^*O_5, \quad (8)$$

where the basis operators are given by

$$O_1 = b, O_2 = b^\dagger, O_3 = a, O_4 = a^\dagger, O_5 = I, \quad (9)$$

and  $f_j$  ( $j = 1 \cdots 5$ ) are time-dependent coefficients. Substituting Eq. (8) to Eq. (7), the differential equations for the coefficients in the  $O$  operator can be determined as

$$\begin{aligned} \frac{\partial}{\partial t}f_1(t, s) &= i\omega_m f_1 + iGf_3 - iGf_4 + f_1F_1, \\ \frac{\partial}{\partial t}f_2(t, s) &= -i\omega_m f_2 + iGf_3 - iGf_4 - f_2F_1 \\ &\quad + 2f_1F_2 - f_4F_3 + f_3F_4 - F_5', \\ \frac{\partial}{\partial t}f_3(t, s) &= -i\Delta f_3 + iGf_1 - iGf_2 + f_1F_3, \\ \frac{\partial}{\partial t}f_4(t, s) &= i\Delta f_4 + iGf_1 - iGf_2 + f_1F_4, \\ \frac{\partial}{\partial t}f_5(t, s, s') &= f_1F_5'(t, s'), \end{aligned} \quad (10)$$

where  $F_j(t) = \int_0^t ds \alpha(t, s)f_j(t, s)$  ( $j = 1 \cdots 4$ ) and  $F_5'(t, s') = \int_0^t ds \alpha(t, s)f_5(t, s, s')$ . The boundary conditions are given by

$$\begin{aligned} f_1(t, s = t) &= 1, \\ f_2(t, s = t) &= f_3(t, s = t) = f_4(t, s = t) = 0, \\ f_5(t, s = t, s') &= 0, \\ f_5(t, s, s' = t) &= f_2(t, s). \end{aligned} \quad (11)$$

In Eq. (5), the non-Markovian properties are reflected by the correlation function. If the correlation is  $\alpha(t, s) = \delta(t, s)$ ,  $\bar{O}$  is reduced to  $\bar{O} = O_1 = b$ , as a result, Eq. (5) is reduced to the Markov quantum trajectory equation investigated in Refs. [53, 54]. Clearly, the additional terms  $O_i$  ( $i = 2, 3, 4, 5$ ) contribute to the non-Markovian corrections. In Fig. 2, we plot the time evolution of the time-dependent coefficients  $F_i$  ( $i = 1, 2, 3, 4$ ) and  $F_5(t) = \int_0^t ds' \alpha(t, s')F_5'(t, s')$ . From the right panel of Fig. 2, when  $\gamma$  is increased, the environment is approaching the well-known Markov limit, hence, the non-Markovian corrections  $F_i$  ( $i = 2, 3, 4, 5$ ) are becoming ignorable. On the contrary, in the case of small  $\gamma$  as plotted in the left panel of Fig. 2, the non-Markovian

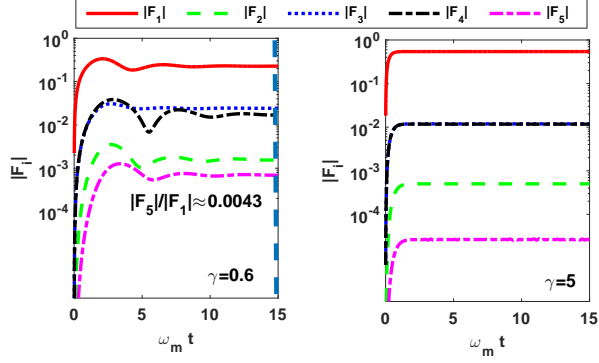


Figure 2. (color online) Time evolution of the coefficients in  $O$  operator. For the case  $\gamma = 0.6$ ,  $\frac{|F_5|}{|F_1|} \approx 0.43\%$  at  $\omega_m t = 15$ .

corrections  $F_i$  ( $i = 3, 4$ ) become more notable compared with the right panel. Fig. 2 roughly shows the corrections to the Markov case caused by the finite memory time and the transition from non-Markovian to Markov regimes. Clearly, the non-Markovian environment not only causes the additional terms  $O_i$  ( $i = 2, 3, 4, 5$ ), but also changes the dynamical behavior especially in the early stage of the evolution. Compared with the right panel, we see that the left panel exhibits some transient oscillation in early stage. This oscillatory evolution directly represents the information exchange between the system and its environment due to the memory effect. In the Markov limit, the environment typically make the system converge to a steady state quickly. As an interesting observation, our discussions later in the paper show that these oscillations eventually result in different entanglement generations. It is also notable that in both panels of Fig. 2, the fifth term  $F_5$  always gives the smallest correction. Hence, this term might be dropped in an approximation approach.

For the purpose of numerical simulation, one can directly simulate the NMQSD equation (5) together with the  $O$  operator given in equation (8). Repeatedly solving equation (5) with stochastic noise  $z_t^*$  and taking the statistical mean of all the generated trajectories, the reduced density matrix can be recovered as

$$\rho_t = M[|\psi_t(z^*)\rangle\langle\psi_t(z^*)|]. \quad (12)$$

The advantage of using this pure state stochastic trajectories approach is the required computational resource is reduced from  $N^2$  (to storage density matrix) to  $N$  (to storage pure state vector). Alternatively, one can also use the NMQSD equation to derive the corresponding exact master equation for the system by following the method in Ref. [40, 48]. In this paper, we will take a straightforward step to truncate the  $O$  operator to the noise free terms, called the zeroth order approximation, which turns out to be appropriate for many practical purposes as discussed in Ref. [49]. Here, as shown before, the fifth term is typically much smaller than the other four terms, so we take the first four terms of the  $O$  operator

as an approximate  $O$  operator

$$O(t, s, z^*) \approx O^{(0)}(t, s) = \sum_{j=1}^4 f_j(t, s) O_j. \quad (13)$$

More systematic discussions on the validity of this approximation has been discussed in Ref. [49]. The corrections from the rest terms with stochastic variable usually contributes up to the fourth order of the coupling strength  $g_j$  [49]. When  $g_j \ll \omega_m$ , the higher order corrections are negligible. Moreover, it is shown quite clearly in Fig. 2 that the contribution of  $F_5$  are always negligible even in the non-Markovian case. With the noise-free  $O$  operator above (13), the master equation takes a very simple form as

$$\begin{aligned} \frac{d}{dt}\rho = & i\Delta(a^\dagger a\rho - \rho a^\dagger a) - i\omega_m(b^\dagger b\rho - \rho b^\dagger b) \\ & -iG(b^\dagger a^\dagger \rho - \rho b^\dagger a^\dagger) - iG(b^\dagger a\rho - \rho b^\dagger a) \\ & -iG(ba^\dagger \rho - \rho ba^\dagger) - iG(ba\rho - \rho ba) \\ & +\{F_1^*(b\rho b^\dagger - \rho b^\dagger b) + F_2^*(b\rho b - \rho bb) \\ & +F_3^*(b\rho a^\dagger - \rho a^\dagger b) + F_4^*(b\rho a - \rho ab) + H.c.\}. \quad (14) \end{aligned}$$

It should be noted that the derivation of the master equation is also irrespective of the format of the correlation function  $\alpha(t, s)$ , namely, the master equation here is applicable to an arbitrary correlation function. As we have discussed, when  $\alpha(t, s) = \delta(t, s)$  (setting  $\Gamma = 1$ ), it is straightforward to show that  $F_1(t) = 0.5$  while  $F_j(t) = 0$  ( $j = 2, 3, 4, 5$ ) [See Eq. (10) and (11)]. Therefore,  $O(t, s) = b$ , and equation (4) is reduced to the traditional Markov quantum trajectory equation [53, 54]. Correspondingly, in the master equation (14) with  $O = b$  is reduced to

$$\frac{d}{dt}\rho = -i[H_S, \rho] + \{[b, \rho b^\dagger] + H.c.\}. \quad (15)$$

This is just the standard Lindblad master equation obtained in the Markov approximation [30].

### III. NUMERICAL RESULTS AND DISCUSSIONS

Solving the optomechanical model by the above non-Markovian approaches, we are capable of analyzing the properties of the entanglement between the cavity field and movable mirror in a non-Markovian regime. For a continuous variable system, several separability criteria exist [55–57]. Here, we will employ the logarithmic negativity [57] to measure the optomechanical entanglement. For a two-mode Gaussian state, it is convenient to write down the momentum operator  $p$  and the position operator  $q$  in a vector form as

$$\xi = (q_1, p_1, q_2, p_2), \quad (16)$$

where  $p_1 = -i(a - a^\dagger)$ ,  $q_1 = (a + a^\dagger)$ ,  $p_2 = -i(b - b^\dagger)$ ,  $q_2 = (b + b^\dagger)$ . Then the commutation relations can be written as

$$[\xi_\alpha, \xi_\beta] = 2iM_{\alpha\beta}, \quad (17)$$

where

$$M = \begin{bmatrix} J & 0 \\ 0 & J \end{bmatrix}, \quad J = \begin{bmatrix} 0 & 1 \\ -1 & 0 \end{bmatrix}. \quad (18)$$

The entanglement properties of the two-mode Gaussian state are completely determined by the variance matrix  $V$  which is defined as

$$V_{\alpha\beta} = \langle \{\Delta\xi_\alpha, \Delta\xi_\beta\} \rangle = \langle (\Delta\xi_\alpha \Delta\xi_\beta + \Delta\xi_\beta \Delta\xi_\alpha) / 2 \rangle, \quad (19)$$

where  $\Delta\xi_\alpha = \xi_\alpha - \langle \xi_\alpha \rangle$ . The variance matrix can be written in a block form as

$$V = \begin{bmatrix} A & C \\ C^T & B \end{bmatrix}. \quad (20)$$

Finally, the logarithmic negativity is defined as

$$En(V) = \max[0, -\ln \nu_-], \quad (21)$$

where  $\nu_-$  is the smallest eigenvalue of the variance matrix  $V$ , which can be computed as

$$\nu_- = \sqrt{[\Sigma(V) - \sqrt{\Sigma(V)^2 - 4 \det V}] / 2}, \quad (22)$$

and  $\Sigma(V) = \det A + \det B - 2 \det C$ .

In order to compute the logarithmic negativity, we need to compute a set of mean values of operators by using the non-Markovian master equation or NMQSD equation,

$$\frac{d}{dt} \langle A \rangle = \frac{d}{dt} M[\langle \psi_t(z^*) | A | \psi_t(z^*) \rangle] = \text{tr}(A \frac{d}{dt} \rho). \quad (23)$$

For this particular model, it is more straightforward to use the derived master equation. However, we pointed out that we can always use the NMQSD equation without deriving the corresponding master equation. The details of the equations for the mean values of operators can be found in the Appendixes.

### A. Memory enhanced entanglement generation

The memory modulated entanglement dynamics is an interesting problem recently [59–62]. Therefore, it is desirable to examine how the environmental parameters  $\gamma$ ,  $\Omega$  affect the entanglement generation between the optical field and the mechanical mode. Fig. 3 shows the dynamics of the entanglement  $En$  with different memory times. As a comparison, the Markov evolution is also plotted in the figure by setting the correlation function  $\alpha(t, s)$  as  $\delta(t, s)$ . It should be noted that according to Fig. 3, we see that a longer memory time (small  $\gamma$ ) will

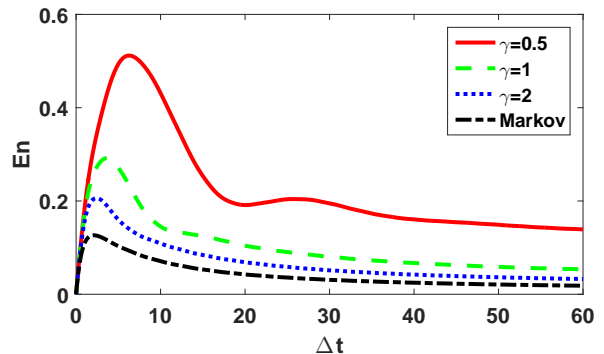


Figure 3. (color online) Memory effect enhanced entanglement generation. The red (solid), green (dashed), and blue (dotted) lines are plotted with different memory times  $1/\gamma$ . The other parameters are chosen as  $\omega_m = 1$ ,  $\Delta = 1$ ,  $G = 0.1$ ,  $\Omega = 0$ ,  $\Gamma = 2$ . The initial state is chosen as  $|\psi_i\rangle = |00\rangle$ . As a comparison, the Markov case is also plotted as the black (dash-dotted) line.

cause a faster entanglement generation. Meanwhile, it is found the longer memory times, the longer duration of the optomechanical entanglement. Since the major decoherence agent of this model is the amplitude damping, the environmental memory plays a role of slowing down the dissipative process due to the back reaction or information back flow. Therefore, one expects that the dissipative dynamics will experience temporal revivals due to the memory effect. On the contrary, the Markov environment causes the system excitations to decay into the environment exponentially without any information back flow. More importantly, the non-Markovian properties of the environment may also affect the residue entanglement in the steady state ( $t \rightarrow \infty$ ). From Fig. 3, a longer memory time give rise to higher residue entanglement degree in a long-time limit. The Markov steady state entanglement in an optomechanical system is discussed in many references such like [22]. In the non-Markovian case considered in this paper, our results show that the dissipation and the back flow from the environment may reach a new balance so that the steady entanglement has a memory of its history. Namely, the steady entanglement may be dependent on the environmental memory time. This finding may be understood from the fact the steady states of a non-Markovian dynamical system are sensitively dependent on the environmental memory parameter  $\gamma$ . In summary, as seen in the numerical simulations, the environmental memory can significantly affect the entanglement generation in both the short-time and long-time limits.

### B. Environmental central frequency and entanglement generation

Apart from the memory time, another important feature of the environment is dictated by the environmen-

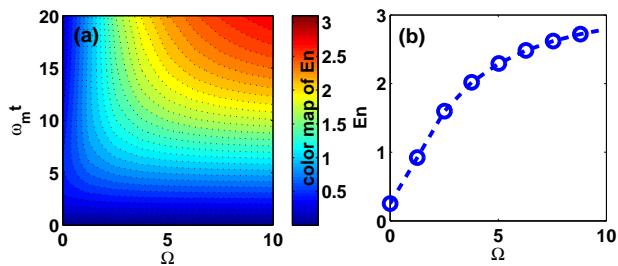


Figure 4. (color online) Time evolution of entanglement for different  $\Omega$ . The left contour plot (a) is the time evolution of the entanglement indicator  $En$  for various values of  $\Omega$ . The right 2-D panel (b) is the entanglement generation for different  $\Omega$  at the fixed time  $\omega_m t = 20$ . The initial state is chosen as  $|\psi_i\rangle = |00\rangle$ . The other parameters are chosen as  $\omega_m = 1$ ,  $\Delta = 1$ ,  $G = 0.1$ , and  $\gamma = 1$ .

tal central frequency  $\Omega$ , which is shown to be important to the entanglement generation [49]. In Fig. 4, we plot the time evolution of entanglement for different  $\Omega$ . The numerical results show that a large  $\Omega$  is useful in generating the optomechanical entanglement. The parameter  $\Omega$  indicates the oscillation frequency of the correlation function  $\alpha(t, s) = \frac{\Gamma\gamma}{2} e^{-(\gamma+i\Omega)|t-s|}$ . A larger  $\Omega$  gives rise to a faster oscillation. Therefore, it explains why a large  $\Omega$  can help to preserve the entanglement since the system is less sensitive to the high-frequency random noise (i.e., when  $\Omega$  is large). Therefore, the high frequency oscillation effectively causes less entanglement degradation after the cavity-mirror entanglement is formed. It is worth to note that this phenomenon can be only observed in non-Markovian case. In the Markov limit,  $\alpha(t, s) = \delta(t, s)$ , the  $O$  operator becomes a time-independent function with constant coefficients. This is an important feature showing the remarkable difference between the non-Markovian and Markov cases. In the non-Markovian case, the information backflow from the environment to the system can effectively protect the entanglement, while in the Markov case the dissipation is monotonic, and the information once dissipated into environment will never come back to the system of interest.

In an experiment context, a new engineering technique about simulating a non-Markovian environment shed a new light on controlling the environment memory effect [35]. This new findings are certainly of interest for motivating more theoretical studies on artificial non-Markovian environment. For example, in the precise quantum measurement [36], the probe can be an effective environment with highly non-Markovian features. In a similar fashion, one can view a pseudomode coupled to an external Markov reservoir as an effectively non-Markovian environment.

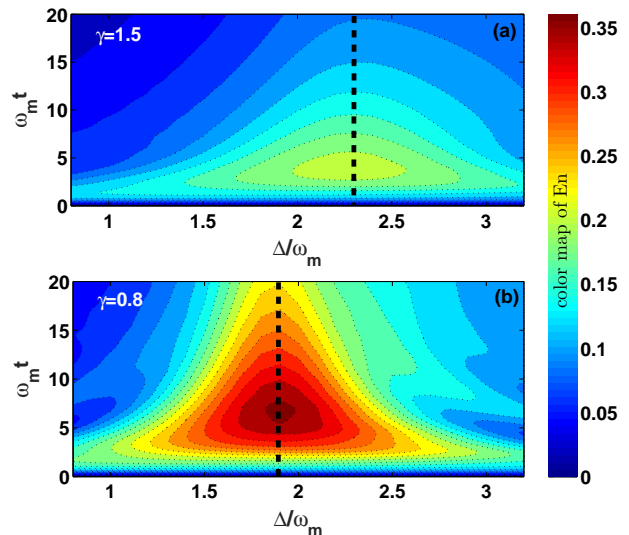


Figure 5. (color online) Time evolution of entanglement for different effective detuning  $\Delta/\omega_m$ . The initial state is chosen as  $|\psi_i\rangle = |00\rangle$ . (a) and (b) are plotted for different memory time  $\gamma = 1.5$  and  $\gamma = 0.8$  respectively. The other parameters are chosen as  $\omega_m = 1$ ,  $\Omega = 0$ ,  $G = 0.1$ , and  $\Gamma = 4$ .

### C. Entanglement generation and the detuning

In Fig. 5, we illustrate the dynamics of the entanglement as the function of effective laser detuning  $\Delta$  and  $\omega_m t$ . Comparing with the environmental spectrum, the driving laser detuning is a more convenient parameter that is effectively controllable. In order to achieve the maximum entanglement generation, one needs to adjust the effective detuning properly. More importantly, the choice of effective detuning substantially depends on the non-Markovian properties of the environment. As illustrated in Fig. 5 (a), when the memory effect parameter  $\gamma = 1.5$  (relatively weak non-Markovian case), the maximum entanglement appears at  $\Delta/\omega_m \approx 2.3$ . As a comparison, in Fig. 5 (b), when the memory effect parameter  $\gamma = 0.8$  (relatively strong non-Markovian), the maximum entanglement appears at  $\Delta/\omega_m \approx 1.9$ . The multiple-dependance of the entanglement generation on the parameters  $\Delta$  and  $\omega$  shows that the optimal entanglement generation in an experiment may benefit from the detailed analysis of the parameter space. Given the non-Markovian environment, one needs to choose a suitable laser detuning in order to generate the maximum entanglement. It was shown in Ref. [22], the choice of effective laser detuning depends on several parameters of the optomechanical system. Here, we emphasize that the non-Markovian properties is also an important factor that can significantly affect the choice of effective detuning. The results in Fig. 5 may prove to be useful in the future when an experiment on generating optomechanical entanglement in non-Markovian environment is conducted.

#### IV. CONCLUSION AND SUMMARY

The recent progress in the experiment has shown that the optomechanical system can be realized in several interesting settings including the traditional cavity-QED systems as well as some artificial circuit-QED systems [63]. More remarkably, with the development of new technology, the environment can be engineered to purposely control the properties of the desired quantum entanglement [35]. Thus, it is useful to develop a versatile theoretical protocols to manipulate entanglement based on the non-Markovian features of the environment.

Our presented results show that the entanglement of the optomechanical system can be strongly affected by several features dictated by a non-Markovian environment. As we showed in Fig. 3 and Fig. 4, the entanglement dynamics of the optomechanical system is sensitively dependent on the choice of the model parameters. And the optomechanical entanglement can be generated in many different ways sensibly depending on the correlation time and the environmental central frequency as well as the the detuning. Our analysis is not expected to unveil all interesting aspects of the environment effect on the optomechanical systems. Rather, our current research should be regarded as an attempt to incorporate the environment memory effects in a more systematic way. Indeed, as shown in this paper, the standard Markov approximation is not adequate for many interesting physical systems. This is particularly important for the macroscopic system as the decoherence time could be comparable with the Markov time, so the Markov approximations deemed to be inadequate when the temporal behaviors of entanglement is of interest. We show that the residue entanglement for the non-Markovian cases can be distinctively different from the Markov steady state.

In summary, we have presented a proposal to entangle a macroscopic vibrating mirror with a cavity field by taking the environment memory effects into account. We show how to use the NMQSD method to solve the model involving an optomechanical system coupled to a non-Markovian environment. In particular, entanglement generation and duration are fully investigated in non-Markovian regimes. We conclude by pointing out a further research is currently being conducted on the physical models where the quantum system-bath coupling is beyond RWA approximation.

#### ACKNOWLEDGMENTS

We acknowledge grant support from DOD/AF/AFOSR No. FA9550-12-1-0001. The research was also supported by the National Natural Science Foundation of China (Grant No. 11205056 & No. 11204078) and the Fundamental Research Funds for the Central Universities (Grant No. 2014ZZD10 & No. 2015MS55).

#### Appendix A: Optomechanical system with both cavity leakage and thermal damping of the mirror

Here, we consider a general case that contains all the possible decoherence mechanism of the system, namely, the  $L$  operator in Eq. (3) can be written as  $L = a + b$ . In order to incorporate the finite-temperature bath, we can transform the finite temperature case into an effective zero temperature model by introducing a fictitious bath [41]. The initial state of the bath for finite temperature case is in the thermal equilibrium state  $\rho_B(0) = \frac{e^{-\beta H_B}}{Z}$ , where  $Z = \text{tr}[e^{-\beta H_B}]$  is the partition function with  $\beta = 1/k_B T$ . The occupation number for mode  $k$  should be

$$\langle c_k^\dagger c_k \rangle = \bar{n}_k = \frac{1}{e^{-\beta \omega_k} - 1}, \quad (\text{A1})$$

which is the well known Bose-Einstein distribution. By introducing a fictitious bath  $H_C = -\sum_k \omega_k c_k^\dagger c_k'$ , without direct interaction with the system and the real bath  $H_B$ , it is possible to map the finite temperature problem into a zero temperature problem with two individual baths. Under the Bogoliubov transformation

$$c_k = \sqrt{\bar{n}_k + 1} d_k + \sqrt{\bar{n}_k} e_k^\dagger, \quad (\text{A2})$$

$$c_k' = \sqrt{\bar{n}_k + 1} e_k + \sqrt{\bar{n}_k} d_k^\dagger, \quad (\text{A3})$$

it is easy to check the vacuum state  $|0\rangle = |0\rangle_d \otimes |0\rangle_e$  satisfies  $\langle 0|_d \langle 0|_e c_k^\dagger c_k |0\rangle_d |0\rangle_e = \bar{n}_k$ . Therefore, solving the original model plus fictitious bath  $H_{tot} = H_S + H_B + H_I + H_C$  with the initial vacuum state  $|0\rangle_d \otimes |0\rangle_e$  is equivalent to solving  $H_S + H_B + H_I$  with the thermal initial state  $\rho_B(0) = e^{-\beta H_B}/Z$ . Now, we need to solve the Hamiltonian in the interaction picture as

$$H_{tot}^{(I)}(t) = H_s + \sum_k (f_k e^{-i\omega_k t} L^\dagger d_k + f_k e^{i\omega_k t} L d_k^\dagger) + \sum_k (h_k e^{-i\omega_k t} L^\dagger e_k^\dagger + h_k e^{i\omega_k t} L e_k), \quad (\text{A4})$$

where  $f_k = \sqrt{\bar{n}_k + 1} g_k$  and  $h_k = \sqrt{\bar{n}_k} g_k$  are the effective coupling constants, and the Lindblad operator is

$$L = a + b, \quad (\text{A5})$$

implying both the cavity leakage and the mirror damping are all taken into consideration.

The non-Markovian NMQSD equation for the finite-temperature case is given by [41],

$$\begin{aligned} \frac{\partial}{\partial t} |\psi(t, z^*, w^*)\rangle &= \left[ -iH_s + Lz_t^* + L^\dagger w_t^* \right. \\ &\quad \left. - L^\dagger \int_0^t ds \alpha_1(t, s) \frac{\delta}{\delta z_s^*} \right. \\ &\quad \left. - L \int_0^t ds \alpha_2(t, s) \frac{\delta}{\delta w_s^*} \right] |\psi(t, z^*, w^*)\rangle, \end{aligned} \quad (\text{A6})$$

where  $z_t^* = -i \sum_k f_k z_k^* e^{i\omega_k t}$ ,  $w_t^* = -i \sum_k h_k^* w_k^* e^{-i\omega_k t}$  are two statistically independent Gaussian noises, and  $\alpha_1(t, s) = \sum_k |f_k|^2 e^{-i\omega_k(t-s)}$  and  $\alpha_2(t, s) = \sum_k |h_k|^2 e^{i\omega_k(t-s)}$  are correlation functions for the two effective baths. Then, we can replace the functional derivatives in Eq. (A6) by two  $O$  operators

$$O_1(t, s, z^*, w^*) |\psi(t, z^*, w^*)\rangle = \frac{\delta}{\delta z_s^*} |\psi(t, z^*, w^*)\rangle, \quad (\text{A7})$$

$$O_2(t, s, z^*, w^*) |\psi(t, z^*, w^*)\rangle = \frac{\delta}{\delta w_s^*} |\psi(t, z^*, w^*)\rangle, \quad (\text{A8})$$

and the  $O$  operators satisfy the following equations,

$$\begin{aligned} \frac{\partial}{\partial t} O_1 &= [-iH_s + Lz_t^* + L^\dagger w_t^* - L^\dagger \bar{O}_1 - L \bar{O}_2, O_1] \\ &\quad - L^\dagger \frac{\delta}{\delta z_s^*} \bar{O}_1 - L \frac{\delta}{\delta z_s^*} \bar{O}_2, \end{aligned} \quad (\text{A9})$$

$$\begin{aligned} \frac{\partial}{\partial t} O_2 &= [-iH_s + Lz_t^* + L^\dagger w_t^* - L^\dagger \bar{O}_1 - L \bar{O}_2, O_2] \\ &\quad - L^\dagger \frac{\delta}{\delta w_s^*} \bar{O}_1 - L \frac{\delta}{\delta w_s^*} \bar{O}_2, \end{aligned} \quad (\text{A10})$$

$$\begin{aligned} O_i(t, s, s') &= x_{i1}(t, s)a + x_{i2}(t, s)a^\dagger + x_{i3}(t, s)b + x_{i4}(t, s)b^\dagger \\ &\quad + \int_0^t y_{i1}(t, s, s') z_s^* ds' + \int_0^t y_{i2}(t, s, s') w_s^* ds' \quad (i = 1, 2), \end{aligned} \quad (\text{A11})$$

$$\begin{aligned} \frac{\partial}{\partial t} x_{i1}(t, s) &= -i\Delta x_{i1} + iGx_{i3} - iGx_{i4} + X_{11}x_{i1} - 2X_{21}x_{i2} + X_{22}x_{i1} \\ &\quad - X_{23}x_{i4} + X_{24}x_{i3} + X_{11}x_{i3} - X_{21}x_{i4} - Y_{2i}(t, s), \end{aligned} \quad (\text{A12})$$

$$\begin{aligned} \frac{\partial}{\partial t} x_{i2}(t, s) &= i\Delta x_{i2} + iGx_{i3} - iGx_{i4} - X_{11}x_{i2} + 2X_{12}x_{i1} - X_{13}x_{i4} \\ &\quad + X_{14}x_{i3} - X_{22}x_{i2} + X_{12}x_{i3} - X_{22}x_{i4} - Y_{1i}(t, s), \end{aligned} \quad (\text{A13})$$

$$\begin{aligned} \frac{\partial}{\partial t} x_{i3}(t, s) &= i\omega_m x_{i3} + iGx_{i1} - iGx_{i2} + X_{13}x_{i1} - X_{23}x_{i2} + X_{13}x_{i3} \\ &\quad - X_{21}x_{i2} + X_{22}x_{i1} - 2X_{23}x_{i4} + X_{24}x_{i3} - Y_{2i}(t, s), \end{aligned} \quad (\text{A14})$$

$$\begin{aligned} \frac{\partial}{\partial t} x_{i4}(t, s) &= -i\omega_m x_{i4} + iGx_{i1} - iGx_{i2} + X_{14}x_{i1} - X_{24}x_{i2} - X_{11}x_{i2} \\ &\quad + X_{12}x_{i1} - X_{13}x_{i4} + 2X_{14}x_{i3} - X_{24}x_{i4} - Y_{1i}(t, s), \end{aligned} \quad (\text{A15})$$

$$\frac{\partial}{\partial t} y_{ik}(t, s, s') = Y_{1k}(t, s')(x_{i1} - x_{i3}) + Y_{2k}(x_{i4} - x_{i2}) \quad (i, k = 1, 2) \quad (\text{A16})$$

where  $X_{ij} = \int_0^t \alpha_i(t, s)x_{ij}(t, s)ds$ , and  $Y_{kl} = \int_0^t \alpha_k(t, s)y_{kl}(t, s, s')ds$ . The boundary conditions for

these equations are:

$$x_{11}(t, t) = x_{13}(t, t) = x_{22}(t, t) = x_{24}(t, t) = 1, \quad (\text{A17})$$

$$x_{12}(t, t) = x_{14}(t, t) = x_{21}(t, t) = x_{23}(t, t) = 0, \quad (\text{A18})$$

$$y_{ij}(t, t, s') = 0. \quad (\text{A19})$$

$$y_{i1}(t, s, t) = x_{i2}(t, s) + x_{i4}(t, s) \quad (\text{A20})$$

$$y_{i2}(t, s, t) = -x_{i1}(t, s) - x_{i3}(t, s) \quad (\text{A21})$$

Given Eq. (A11-A21),  $O$  operator can be fully determined, therefore Eq. (A6) is solved.

Using Eq. (A6) with the exact  $O$  operator in Eq. (A11), one can also derive a master equation as

$$\begin{aligned} \frac{\partial}{\partial t} \rho_S = & -i[H_S, \rho_S] + [L, M\{P_t \bar{O}_1^\dagger\}] - [L^\dagger, M\{\bar{O}_1 P_t\}] \\ & + [L^\dagger, M\{P_t \bar{O}_2^\dagger\}] - [L, M\{\bar{O}_2 P_t\}], \end{aligned} \quad (\text{A22})$$

where  $P_t \equiv |\psi(t, z^*, w^*)\rangle\langle\psi(t, z, w)|$  is the stochastic density operator. For the details of deriving the master equation, one can follow the examples in Refs. [40, 47, 48].

## Appendix B: Equations for mean values

In this section, we show the methods we have used to compute the evolution of the entanglement. According to Eq. (14) and Eq. (23), the equations for the mean values of the operators can be obtained as

$$\frac{d}{dt} \langle b \rangle = -i\omega_m \langle b \rangle - iG \langle a^\dagger \rangle - iG \langle a \rangle - \sum_{i=1}^4 F_i \langle O_i \rangle \quad (\text{B1})$$

$$\frac{d}{dt} \langle b^\dagger \rangle = i\omega_m \langle b^\dagger \rangle + iG \langle a^\dagger \rangle + iG \langle a \rangle - \sum_{i=1}^4 F_i^* \langle O_i^\dagger \rangle \quad (\text{B2})$$

$$\frac{d}{dt} \langle a \rangle = i\Delta \langle a \rangle - iG \langle b^\dagger \rangle - iG \langle b \rangle \quad (\text{B3})$$

$$\frac{d}{dt} \langle a^\dagger \rangle = -i\Delta \langle a^\dagger \rangle + iG \langle b^\dagger \rangle + iG \langle b \rangle \quad (\text{B4})$$

$$\frac{d}{dt} \langle aa \rangle = 2i\Delta \langle aa \rangle - 2iG \langle ab^\dagger \rangle - 2iG \langle ab \rangle \quad (\text{B5})$$

$$\frac{d}{dt} \langle aa^\dagger \rangle = iG \langle ab^\dagger \rangle + iG \langle ab \rangle - iG \langle a^\dagger b^\dagger \rangle - iG \langle a^\dagger b \rangle \quad (\text{B6})$$

$$\begin{aligned} \frac{d}{dt} \langle ab \rangle = & i\Delta \langle ab \rangle - i\omega_m \langle ab \rangle - iG(\langle aa^\dagger \rangle + \langle bb^\dagger \rangle - 1) \\ & - iG \langle aa \rangle - iG \langle bb \rangle - \sum_{i=1}^4 F_i \langle a O_i \rangle \end{aligned} \quad (\text{B7})$$

$$\begin{aligned} \frac{d}{dt} \langle ab^\dagger \rangle = & i\Delta \langle ab^\dagger \rangle + i\omega_m \langle ab^\dagger \rangle - iG \langle b^\dagger b^\dagger \rangle - iG(\langle bb^\dagger \rangle \\ & - \langle aa^\dagger \rangle) + iG \langle aa \rangle - \sum_{i=1}^4 F_i^* \langle O_i^\dagger a \rangle \end{aligned} \quad (\text{B8})$$

$$\frac{d}{dt} \langle a^\dagger a^\dagger \rangle = -2i\Delta \langle a^\dagger a^\dagger \rangle + 2iG \langle a^\dagger b^\dagger \rangle + 2iG \langle a^\dagger b \rangle \quad (\text{B9})$$

$$\begin{aligned} \frac{d}{dt} \langle a^\dagger b \rangle = & -i\Delta \langle a^\dagger b \rangle - i\omega_m \langle a^\dagger b \rangle - iG \langle a^\dagger a^\dagger \rangle - iG(\langle aa^\dagger \rangle \\ & - \langle bb^\dagger \rangle) + iG \langle bb \rangle - \sum_{i=1}^4 F_i \langle a^\dagger O_i \rangle \end{aligned} \quad (\text{B10})$$

$$\frac{d}{dt} \langle a^\dagger b^\dagger \rangle = \left[ \frac{d}{dt} \langle ab \rangle \right]^\dagger \quad (\text{B11})$$

$$\frac{d}{dt} \langle bb \rangle = -2i\omega_m \langle bb \rangle - 2iG \langle a^\dagger b \rangle - 2iG \langle ab \rangle - \sum_{i=1}^4 2F_i \langle b O_i \rangle \quad (\text{B12})$$

$$\begin{aligned} \frac{d}{dt} \langle bb^\dagger \rangle = & -iG \langle a^\dagger b^\dagger \rangle - iG \langle ab^\dagger \rangle + iG \langle a^\dagger b \rangle + iG \langle ab \rangle \\ & - \left\{ \sum_{i=1}^4 F_i^* \langle O_i^\dagger b \rangle + H.c. \right\} \end{aligned} \quad (\text{B13})$$

$$\begin{aligned} \frac{d}{dt} \langle b^\dagger b^\dagger \rangle = & 2i\omega_m \langle b^\dagger b^\dagger \rangle + 2iG \langle ab^\dagger \rangle + 2iG \langle a^\dagger b^\dagger \rangle \\ & - \sum_{i=1}^4 2F_i^* \langle O_i^\dagger b^\dagger \rangle \end{aligned} \quad (\text{B14})$$

With the equations above, the  $V$  matrix as well as the entanglement can be computed.

- 
- [1] E. Schrödinger, *Naturwissenschaften* **23**, 807 (1935).  
 [2] S. Pirandola, D. Vitali, P. Tombesi, and S. Lloyd, *Phys. Rev. Lett.* **97**, 150403 (2006).  
 [3] F. Plastina, R. Fazio, and G. M. Palma, *Phys. Rev. B* **64**, 113306 (2001).

- [4] W. Dür and H.-J. Briegel, *Phys. Rev. Lett.* **92**, 180403 (2004).  
 [5] H. Krauter *et al.*, *Phys. Rev. Lett.* **107**, 080503 (2011).  
 [6] P. Sekatski, M. Aspelmeyer, and N. Sangouard, *Phys. Rev. Lett.* **112**, 080502 (2014).

- [7] S. Mancini, V. Giovannetti, D. Vitali, and P. Tombesi, *Phys. Rev. Lett.* **88**, 120401 (2002).
- [8] L. Zhou, H. Xiong, and M. S. Zubairy, *Phys. Rev. A* **74**, 022321 (2006).
- [9] X.-Y. Zhao, Y.-H. Ma, and L. Zhou, *Opt. Commun.* **282**, 1593 (2009).
- [10] S. Bose, K. Jacobs, and P. L. Knight, *Phys. Rev. A* **59**, 3204 (1999).
- [11] S. Mancini, V. I. Man'ko, and P. Tombesi, *Phys. Rev. A* **55**, 3042 (1997).
- [12] C.-H. Chou, T. Yu, and B. L. Hu, *Phys. Rev. E* **77**, 011112 (2008).
- [13] C. H. Chou, B. L. Hu, and T. Yu, *Physica A* **387**, 432 (2008).
- [14] K. C. Schwab, and M. L. Roukes, *Phys. Today* **58**, 36 (2005).
- [15] W. H. Zurek, *Phys. Today* **44** (10), 36 (1991).
- [16] S. Gröblacher, K. Hammerer, M. R. Vanner, and M. Aspelmeyer, *Nature* **460**, 724 (2009).
- [17] J. Teufel *et al.*, *Nature (London)* **475**, 359 (2011).
- [18] T. A. Palomaki, J. D. Teufel, R. W. Simmonds, and K. W. Lehnert, *Science* **342**, 710 (2013).
- [19] S. Mancini, D. Vitali, and P. Tombesi, *Phys. Rev. Lett.* **80**, 688 (1998).
- [20] M. Aspelmeyer, T. J. Kippenberg, and F. Marquardt, *Rev. Mod. Phys.* **86**, 1391 (2014).
- [21] W. Marshall, C. Simon, R. Penrose, and D. Bouwmeester, *Phys. Rev. Lett.* **91**, 130401 (2003).
- [22] D. Vitali *et al.*, *Phys. Rev. Lett.* **98**, 030405 (2007).
- [23] Y. Chen, *J. Phys. B* **46**, 104001 (2013).
- [24] C. Genes, A. Mari, P. Tombesi, and D. Vitali, *Phys. Rev. A* **78**, 032316 (2008).
- [25] A. Nunnenkamp, K. Borkje, and S. M. Girvin, *Phys. Rev. Lett.* **107**, 063602 (2011).
- [26] P. Meystre, *Ann. Phys. (Berlin)* **525**, 215 (2013).
- [27] K. Zhang, F. Bariani, and P. Meystre, *Phys. Rev. Lett.* **112**, 150602 (2014).
- [28] R. Ghobadi, S. Kumar, B. Pepper, D. Bouwmeester, A. I. Lvovsky, and C. Simon, *Phys. Rev. Lett.* **112**, 080503 (2014).
- [29] G. Wang, L. Huang, Y.-C. Lai, and C. Grebogi, *Phys. Rev. Lett.* **112**, 110406 (2014).
- [30] H.-P. Breuer and F. Petruccione, *The Theory of Open Quantum Systems* (Oxford University Press, Oxford, 2002).
- [31] J. P. Paz, *Phys. Rev. Lett.* **100**, 220401 (2008).
- [32] Y.-D. Wang and A. A. Clerk, *Phys. Rev. Lett.* **110**, 253601 (2013).
- [33] S. Gröblacher, A. Trubarov, N. Prigge, G. D. Cole, M. Aspelmeyer, and J. Eisert, *Nat. Commu.* **6**, 7606 (2015).
- [34] J. Cheng, W. Z. Zhang, L. Zhou, and W. Zhang, *Sci. Rep.* **6**, 23678 (2016).
- [35] B.-H. Liu, L. Li, Y.-F. Huang, C.-F. Li, G.-C. Guo, E.-M. Laine, H.-P. Breuer, and J. Piilo, *Nat. Phys.* **7**, 931 (2011).
- [36] H. Yang, H. Miao, and Y. Chen, *Phys. Rev. A* **85**, 040101(R) (2012).
- [37] L. Diósi, N. Gisin, and W. T. Strunz, *Phys. Rev. A* **58**, 1699 (1998).
- [38] W. T. Strunz, L. Diósi, and N. Gisin, *Phys. Rev. Lett.* **82**, 1801 (1999).
- [39] T. Yu, L. Diósi, N. Gisin, and W. T. Strunz, *Phys. Rev. A* **60**, 91 (1999).
- [40] W. T. Strunz and T. Yu, *Phys. Rev. A* **69**, 052115 (2004).
- [41] T. Yu, *Phys. Rev. A* **69**, 062107 (2004).
- [42] J. Jing and T. Yu, *Phys. Rev. Lett.* **105**, 240403 (2010).
- [43] X. Zhao, J. Jing, B. Corn, and T. Yu, *Phys. Rev. A* **84**, 032101 (2011).
- [44] X. Zhao, W. Shi, L.-A. Wu, and T. Yu, *Phys. Rev. A* **86**, 032116 (2012).
- [45] W. Shi, X. Zhao, and T. Yu, *Phys. Rev. A* **87**, 052127 (2013).
- [46] M. Chen, and J. Q. You, *Phys. Rev. A* **87**, 052108 (2013).
- [47] X. Zhao, J. Jing, J. Q. You, and T. Yu, *Quantum Inf. and Compu.* **14**, 0741 (2014).
- [48] Y. Chen, J. Q. You, and T. Yu, *Phys. Rev. A* **90**, 052104 (2014).
- [49] J. Xu, X. Zhao, J. Jing, L.-A. Wu, and T. Yu, *J. Phys. A* **47**, 435301 (2014).
- [50] C. K. Law, *Phys. Rev. A* **49**, 433 (1994).
- [51] C. Joshi, P. Öhberg, J. D. Cresser, and E. Andersson, *Phys. Rev. A* **90**, 063815 (2014).
- [52] J. D. Cresser, *J. Mod. Opt.* **39**, 2187 (1992).
- [53] J. Dalibard, Y. Castin, and K. Mølmer, *Phys. Rev. Lett.* **68**, 580 (1992).
- [54] N. Gisin and I. C. Percival, *J. Phys. A* **25**, 5677 (1992).
- [55] R. Simon, *Phys. Rev. Lett.* **84**, 2726 (2000).
- [56] L.-M. Duan, G. Giedke, J. I. Cirac, and P. Zoller, *Phys. Rev. Lett.* **84**, 2722 (2000).
- [57] G. Adesso, A. Serafini, and F. Illuminati, *Phys. Rev. A* **70**, 022318 (2004).
- [58] A. H. Safavi-Naeini *et al.*, *New J. Phys.* **15**, 035007 (2013).
- [59] M. B. Plenio and S. F. Huelga, *Phys. Rev. Lett.* **88**, 197901 (2002).
- [60] S. F. Huelga and M. B. Plenio, *Phys. Rev. Lett.* **98**, 170601 (2007).
- [61] N. Lambert, R. Aguado, and T. Brandes, *Phys. Rev. B* **75**, 045340 (2007).
- [62] X. X. Yi, C. S. Yu, L. Zhou, and H. S. Song, *Phys. Rev. A* **68**, 052304 (2003).
- [63] S. Felicetti, *et al.*, *Phys. Rev. Lett.* **113**, 093602 (2014).